THE JOURNAL OF COMPARATIVE NEUROLOGY 304:491–501 (1991)

Labeling and Distribution of AII Amacrine Cells in the Rabbit Retina

STEPHEN L. MILLS AND STEPHEN C. MASSEY
Sensory Sciences Center, Graduate School of Biomedical Sciences, University of Texas Health Science Center, Houston, Texas 77030

ABSTRACT

The fluorescent dye 4,6-diamino-2-phenylindole (DAPI) has previously been used to label starburst amacrine cells selectively in the rabbit retina and AII amacrine cells in the cat retina. Using the rabbit retina, we show that intraocular injection of DAPI labels starburst amacrine cells as seen 1–2 days later. In contrast, after a brief in vitro incubation with DAPI, AII amacrine cells are selectively labeled. Amacrine cells were identified by intracellular staining with Lucifer Yellow. AII amacrine cells are arranged in a regular mosaic with a density of 2,800 cells/mm^2 near the visual streak declining to about 500 cells/mm^2 in the far periphery. The coverage of the lobular dendritic field in sublamina *a* is approximately 1.5 across the retina, but the coverage of the fine dendritic field in sublamina *b* increases from 3 centrally to 4 in the inferior periphery, and to above 8 in the superior periphery.

Key words: 4,6-diamino-2-phenylindole (DAPI), starburst amacrine cells, Lucifer Yellow, rods, coverage factors

The major flow of photopic information through the retina is via a three-neuron chain from cones through cone bipolar cells to ganglion cells. However, the rod pathway is less direct; synapses from rod bipolar cells directly onto ganglion cells are rare (Kolb and Famiglietti, '74; Strettoi et al., '90). Instead, an interneuron, the AII amacrine cell, transmits information from rod bipolar cells to cone bipolar cells and is thus an integral part of the rod pathway.

The AII amacrine cell is a small, distinctly bistratified cell. It has been shown in cat and rabbit retina to receive input from rod bipolar cells deep in sublamina *b* (Famiglietti and Kolb, '75; Sterling, '83; Raviola and Dacheux, '87). The fine processes of AII cells in sublamina *b* not only receive input from rod bipolar cells and other amacrine cells, but they also make electrical contact through gap junctions with ON cone bipolar cells and other AII amacrine cells (McGuire et al., '84, '86; Sterling et al., '88). The lobular appendages in sublamina *a* synapse almost exclusively onto hyperpolarizing cone bipolars (Famiglietti and Kolb, '75; Strettoi et al., '90). AII amacrine cells are depolarized by light (Nelson, '82; Dacheux and Raviola, '86) and they appear to be glycinergic, since they accumulate ^{3}H-glycine (Pourcho and Goebel, '85) and show immunoreactivity for glycine-conjugated molecules in the cat retina (Pourcho and Goebel, '87). Furthermore, the dark-adapted input to OFF ganglion cells, which passes via conventional synapses between AII amacrine cells and OFF bipolar cells, is blocked by the glycine antagonist strychnine (Wässle et al., '86).

A reliable method of visualizing AII amacrine cell somas in cat retina has been described by Vaney ('85), who found that in vitro incubation in 0.5 mg/l of the fluorescent dye 4,6-diamino-2-phenylindole (DAPI) led to selective marking of AII amacrine cells. However, Vaney's method did not preferentially label the AII mosaic in the rabbit retina. This report describes a similar method of labeling AII amacrine cells with DAPI in the rabbit retina and a comparison is made with labeling of starburst amacrine cells by the intravitreal injection method. After labeling, the DAPI-fluorescent somas can be impaled and filled with Lucifer Yellow to reveal their fine dendritic structure (Stewart, '81). From this material, the density and coverage of AII amacrine cells in the rabbit retina have been calculated.

MATERIALS AND METHODS

Intraocular injection

New Zealand White rabbits were anesthetized with a ketamine/acepromazine/xylazine cocktail (3:1:1, 0.25 ml/kg, I.P.) for intraocular injections. The orbit was irrigated with lidocaine hydrochloride and DAPI was injected in 10–50 µl of isotonic saline carrier. Full recovery was obtained after 1 or 2 hours and the eye was enucleated under deep anesthesia 2 or more days later.

Accepted October 16, 1990.

Address reprint requests to Stephen L. Mills, UTHSCH Sensory Sciences, 6420 Lamar Fleming, Rm. 316, Houston, TX 77030.

Retinal preparation

Rabbits were deeply anesthetized with urethane (loading dose, 1.5 g/kg, I.P.) and each eye was removed and hemisected. The eyecup was everted over a rounded Teflon post and suspended in oxygenated medium (Ames and Nesbett, '81) at 37°C. A glass rod was used to tease the retina away from the sclera, taking care to contact the retina itself as little as possible (Tauchi and Masland, '84). After the optic nerve was cut, the retina was then flattened on Whatman 40 filter paper and cut into pieces with a razor blade. Each piece was subsequently placed in a chamber and held stationary with Parafilm and acrylic. An exposed patch of retina was continuously perfused with oxygenated Ames medium.

For incubation in DAPI, the retina was separated from the sclera in oxygenated medium containing 4–8 μM DAPI. Retinal pieces were further incubated in this medium following separation from the sclera for a total incubation time of 45–90 minutes.

Visual identification of somas

A Zeiss microscope modified for fixed stage and fitted with epifluorescence was used to examine pieces of tissue for DAPI labeling. Two filter sets served to illuminate the tissue with wavelengths specific for excitation of DAPI or Lucifer Yellow, and to permit selective transmission of the wavelengths emitted by these dyes upon excitation. Additional trimming filters could be added to enhance contrast of specific features of the tissue sample. The DAPI filter set used an excitation interference filter centered at 365 nm and passed wavelengths above 397 nm for viewing. The Lucifer Yellow filter set had a bandpass of 400–440 nm for excitation and passed wavelengths above 470 nm for viewing.

Lucifer Yellow injection

Cells were impaled under visual control using a long working distance objective (Nikon, SLWD, 40X). Micropipettes were pulled on a Brown-Flaming horizontal micropipette puller (Sutter P-80), tip-filled with 8% Lucifer Yellow-CH (Molecular Probes) in 50 mM Tris and backfilled with 3M lithium chloride. When the cell of interest was contacted by the electrode tip, penetration was forced and Lucifer Yellow ejected with 5 to 25 nA, 6 Hz negative current pulses until the cell was filled (Stewart, '81). Tissue with filled cells was removed from the chamber and fixed in 2% paraformaldehyde and 0–.2% glutaraldehyde for 30 minutes. The lightly fixed tissue used to measure densities and dendritic fields showed minimal shrinkage, usually less than 5%. Greater shrinkage can be expected after photooxidation, dehydration, and embedding, but these preparations were not used for density and size determinations.

Enhancement with DAB and osmication

A disadvantage of fluorescent markers is that they fade with continued exposure to fluorescent light. This drawback can be overcome by treatment with 3,3′-diaminobenzidine (DAB) (Maranto, '82). Irradiation of fluorescent cells for periods of 8–30 minutes produces a dark reaction product. Further improvement of the cell/background ratio can be achieved by treatment of the DAB-reacted cell with an osmication procedure (Karnovsky, '71). The tissue is then dehydrated and embedded in Epon. Cells may then be photographed and drawn without fading. The procedure of Sandell and Masland ('88) was followed closely. For optimal photoconversion, DAB solution was made fresh each day and kept in ice. Maintenance of a pH near 8.2 appeared critical. Rapid photoconversion using the highest powered objective possible produced best results; bright cells converted best.

Analysis

Narrow strips perpendicular to the visual streak were cut from each of several retinas. AII amacrine cells were filled at regular intervals throughout some strips of retina. Population counts were determined by placing a coverslip on a piece of tissue, then using a drawing tube to trace AII amacrine cell somas on a sheet of paper. The drawing area was 140 × 210 μm, 0.0294 mm^2, when viewed through a 40X oil-immersion lens. Dendritic field diameters were measured by comparing injected cells with a calibrated scale viewed through the drawing tube. For asymmetric cells, the average of the long and short axes was used as the field diameter.

Tracings of population densities were also used to determine the orderliness of the AII mosaic. The distance from each cell to its nearest neighbor was measured using a Hewlett-Packard 9111A Graphics Tablet. The ratio of the mean to the standard deviation for a sample provided an index of regularity in distribution (Wässle and Riemann, '78).

Coverage factors were determined by multiplying cell densities in cells/mm^2 by dendritic field areas in mm^2. These were calculated separately for the lobular appendages and fine dendrites of AII amacrine cells.

The dendritic trees of some cells were sketched by use of the drawing tube and the area of their dendritic trees and total length of their dendritic processes measured using a graphics tablet. Samples were taken from extreme superior and inferior periphery, as well as from central and midperipheral retina.

RESULTS

We routinely use intraocular injection of 0.3–6 μg DAPI to label amacrine cells in rabbit retina. Figure 1 shows the regular mosaic of cell bodies produced in the ganglion cell layer by injection of 0.5 μg DAPI. Injection of Lucifer Yellow into these somas reveals the dendritic morphology of starburst amacrine cells, as previously reported (Tauchi and Masland, '84; Vaney, '84). A few somas belonging to ganglion cells are also visible, particularly at higher doses of DAPI. These are easily discriminated from displaced starburst amacrine cells on the basis of size and brightness. Figure 2 shows three starburst amacrine cells from another retina that have been impaled, filled with Lucifer Yellow, fixed, photooxidized, osmicated, and embedded. In retinas labeled with low concentrations of DAPI and viewed 1 or more days postinjection, starburst amacrine cells are the only cells to be brightly labeled, although two other amacrine cell types are dimly visible in the inner nuclear layer (INL) (Tauchi and Masland, '84; Vaney, '84). As concentration is increased, other amacrine cell types also become visible; some of these can be recognized by their brightness, soma size and appearance, and by their depth in the INL.

In our experience, AII amacrine cells have been difficult to identify by intraocular injection of DAPI. Since in vitro incubation with DAPI can label starburst and other amacrine cells and this method has been used to label AII

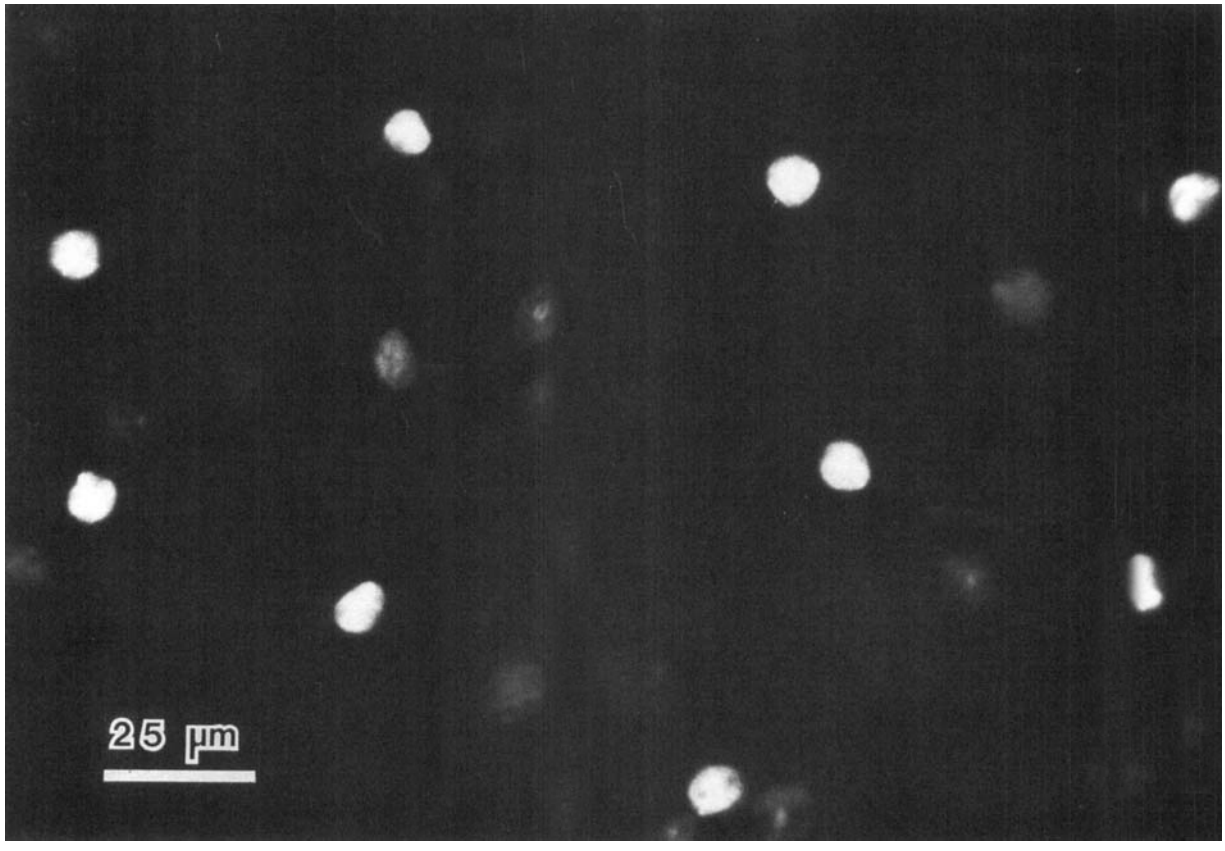

Fig. 1. A fluorescence micrograph (DAPI filter set) showing the matrix of displaced starburst amacrine cells produced by intravitreal injection of 0.5 μg of DAPI 2 days prior to enucleation.

amacrine cells in the cat retina, we conducted a systematic investigation for the rabbit retina. We found that in vitro incubation in 4-μM DAPI labeled a regular mosaic of cells in the INL. These were found upon injection with Lucifer Yellow to be bistratified, with lobular appendages in sublamina *a* and fine processes in sublamina *b*, characteristics diagnostic for AII amacrine cells. The somas were located at the border of the INL and inner plexiform layer (IPL) and, particularly in the periphery, could protrude into the IPL. Figure 3 shows one such array of AII amacrine somas following incubation for 50 minutes in 5-μM DAPI. The tissue was photographed using the DAPI filter set. Although other cells also show some DAPI fluorescence, their lower brightness and different planes of focus permit the AII population to be easily discriminated. Figure 4 shows six AII amacrine cells from a comparable AII matrix in the midperiphery that have been injected with Lucifer Yellow and subsequently photooxidized with DAB and osmicated. Figure 4A is focused on the lobular appendages in sublamina *a*. Figure 4B is focused on sublamina *b* and shows the characteristic fine dendrites of AII amacrine cells in this layer. These cells are not nearest neighbors, but are spaced with one to two somas intervening to permit the identity and dendritic spread of each cell to be seen more clearly. This sequence of photographs demonstrates that DAPI incubation labels a regular matrix of cells identifiable by level of focus and brightness against the more dimly labeled cells in the background and that injection of Lucifer Yellow into these cells reveals them to be AII amacrine cells.

We have found that incubation in 5-μM DAPI for 50 minutes is the most reliable way to label AII amacrine cells selectively. Under incubation conditions that produce ideal labeling of AII amacrine cells, virtually no labeling is seen in the ganglion cell layer. An exception is the bright cell bodies that appear around blood vessels near the myelinated band. After about 90 minutes of incubation, the selectivity shown by the DAPI labeling begins to diminish. Among the cell types that appear after this interval are the displaced starburst amacrine cells. Indoleamine-accumulating cells of the type S1 (A17 in the cat) are often visible as dark somas slightly larger than those of AII amacrine cells. Still longer incubation times lead to the appearance of starburst amacrine cells in the inner nuclear layer. However, under these conditions many other cells are labeled and it is difficult to pick out the starburst amacrine cells reliably. Intraocular injection of DAPI is a superior way to label starburst amacrine cells.

Figure 5 demonstrates the difference in size of AII amacrine cells as a function of retinal eccentricity. The small cell (A) is from within 2 mm of the visual streak; the large cell (B) is from about 10 mm in the periphery of the superior retina. The fine processes in sublamina *b* are shown as filled-in processes; the lobular appendages in sublamina *a* are drawn with stippling. The fine processes are only a little longer than the lobular appendages in the central area but increase more rapidly with eccentricity so that, as can be seen in the large cell, the dendritic field width of the fine processes greatly exceeds that of the

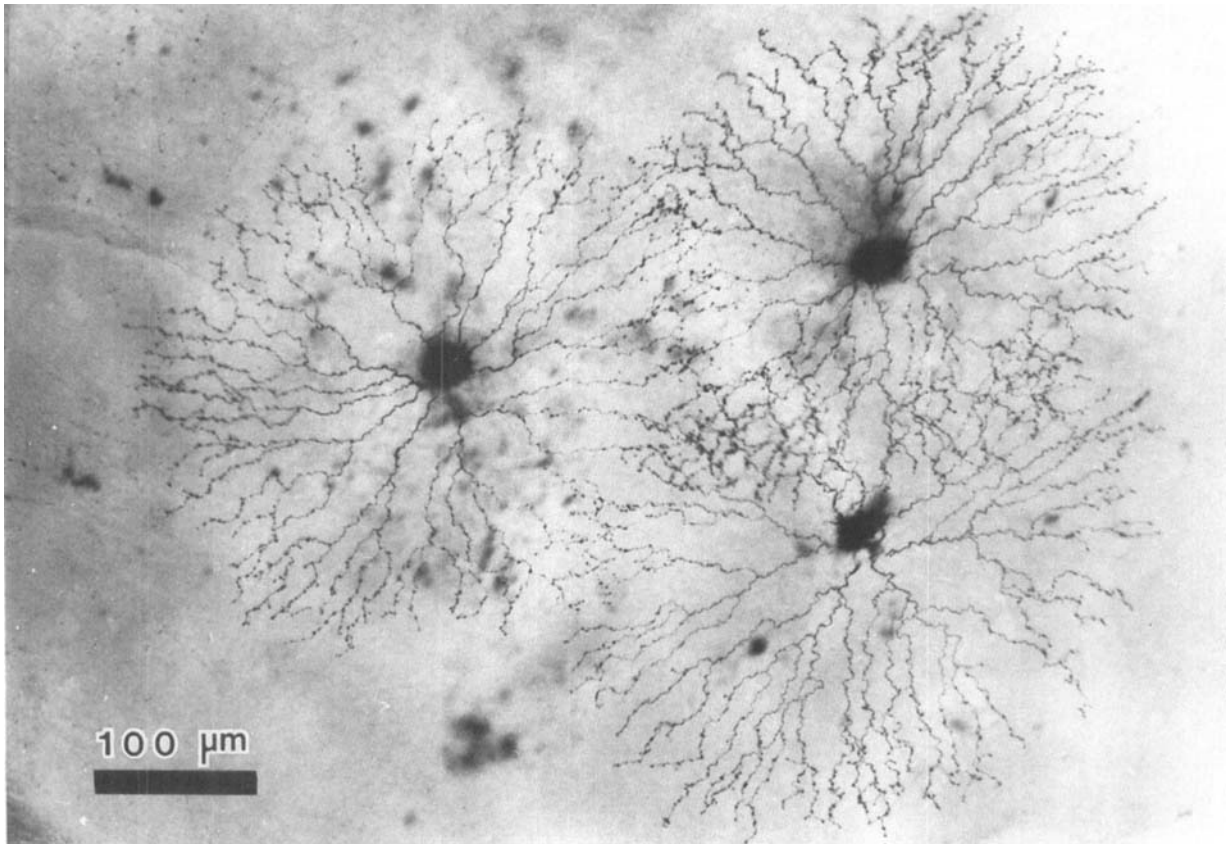

Fig. 2. Three displaced starburst amacrine cells impaled and filled with Lucifer Yellow, then photooxidized and osmicated.

lobular appendages at some locations. Figure 6A shows how the size of these two types of dendritic field increases as a function of eccentricity. The presence of the myelinated band just superior to the visual streak in rabbit retina is reflected in the lack of data points from 1 to 5 mm superior to the visual streak in this and ensuing figures. Smooth lines were drawn by eye through the two sets of data points. Figure 6A shows that the dendritic field width of the lobular appendages (a) increases less rapidly than that of the fine processes (b). Most notable is how the fine processes increase in field diameter in the superior retina. Near the visual streak, both sets of appendages are about 35–45 µm in diameter. In the periphery, the field formed by the lobular appendages increases to about 55 µm, whereas the field of the fine processes averages about 80 µm in the inferior periphery and more than 110 µm in the superior periphery. These processes can occasionally be as large as 200 µm in diameter.

Fluorescent labeling with DAPI may also be used to study the distribution of AII amacrine cells. The general pattern of the AII amacrine cell distribution is similar to that in the cat retina, although total cell density is significantly lower. As shown in Figure 6B, the AII population decreases rapidly from a maximum of about 2,800 cells/mm^2 in the central portion of the visual streak to about 500 cells/mm^2 in the far periphery. This compares with about 5,000–6,000 and 500–800 for analogous locations in the cat retina (Vaney, '85). A smooth line was drawn by eye through the data points from the inferior retina. The reflection of this line about 0° eccentricity is shown as the dashed line in Figure 6B and indicates that cell density falls off more rapidly in superior retina than inferior to the visual streak.

The degree to which AII amacrine cells form a regular mosaic is shown in Figure 6C,D. The lower left panel (C) shows the distribution of AII somas within 1 mm of the visual streak. The lower right panel (D) shows an analogous distribution obtained 18 mm from the central area. Nearest-neighbor analysis (Wässle and Riemann, '78) uses mean/standard deviation ratios of the distance between each cell in the mosaic and its nearest neighbor to indicate the extent to which the distribution deviates from a random distribution containing the same overall cell density. A ratio of 1 indicates a random distribution; a regular lattice with virtually no variation in distance between neighbors would have a very large index. The mosaic of AII amacrine cells in the rabbit retina has a mean/standard deviation ratio of 3.89. This compares with ratios of 2.8 to 3.0 for indoleamine-accumulating cells in the INL of the rabbit (Sandell and Masland, '86) and 3.1 for starburst amacrine cells in the peripheral retina of the rabbit (Masland et al., '84). The larger ratios for AII amacrine cells may be a consequence of their direct involvement in the rod throughout pathway. Irregularities in the matrix would translate into increased spatial uncertainty. These numbers compare to about 5.2 in the cat (Vaney, '85). No differences were found between the index of regularity as a function of retinal eccentricity.

Dendritic field coverage can be calculated by using the densities in Figure 6B and the dendritic field sizes in Figure

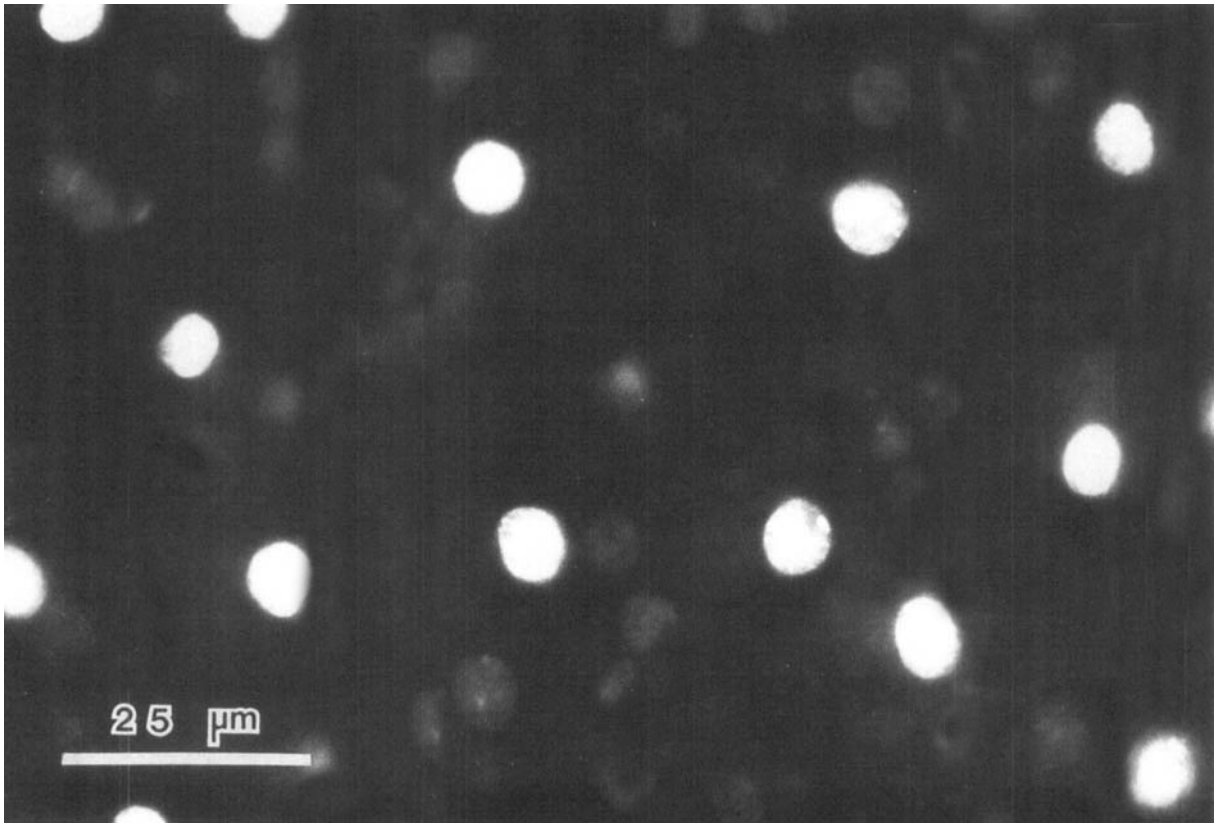

Fig. 3. A fluorescence micrograph (DAPI filter set) showing the matrix of AII amacrine cells somas revealed after incubation in 5 µM DAPI for 50 minutes. The ghosts in the background are weakly labeled amacrine and bipolar cells.

6A. Calculations of coverage factors are naturally higher for sublamina *b* than for sublamina *a*, as a consequence of the increased dendritic field width of the fine processes. Figure 7 shows coverage factors for the lobular appendages (a) and the fine dendrites (b) as a function of eccentricity. Coverage for the lobular appendages is virtually constant across the retina, at 1.5. This simply reflects the increase in field diameter as the cell density falls with eccentricity. The fine dendrites in sublamina *b* have a coverage between 3 and 4 from central to inferior periphery. However, in the superior retina the coverage of the fine dendrites increases to more than 8 as a consequence of the steep increase in field diameter (Fig. 6A).

Figure 8 shows the number of cells within the field of a particular AII amacrine cell taken from the superior periphery at an eccentricity of 10 mm. Figure 8A is focused on the lobular appendages in sublamina *a* and Figure 8B shows the fine dendrites in sublamina *b*. The mosaic of AII amacrine cell somas overlapping these fields is shown in Figure 8C. Comparison of C with the prior two panels shows that the fine dendritic field of this AII amacrine cell contains somas from about 6 adjacent AII amacrine cells. This is illustrated most clearly by the schematic drawing in Figure 8D, where the position of the surrounding AII amacrine cell somas is shown relative to the impaled cell. The offset field formed by the lobules of this particular cell cover no other AII amacrine cell somas, but in general, the lobular field can be expected to contain a nearby soma.

DISCUSSION

By intracellular staining with Lucifer Yellow, we have determined which amacrine cells in the rabbit retina are labeled with the fluorescent dye DAPI. Our results lead to three major conclusions: (1) AII amacrine cells may be selectively labeled in brief in vitro incubations in DAPI; starburst amacrine cells appear after longer incubation times or intraocular injections performed several hours or days before enucleation, (2) differences in cell populations labeled by DAPI appear to be a result of time-dependent labeling, rather than solely a species difference, and (3) the distribution of AII amacrine cells in the rabbit is similar to that of the cat, but the overall density is lower.

Labeling specificity

Selective labeling of the AII amacrine cell matrix is a valuable technique that should facilitate further study of these cells in the rabbit retina, including detailed microscopy, autoradiography, and dye coupling. The data presented above demonstrate that AII amacrine cells can be preferentially labeled in the rabbit retina as well as in the cat (Vaney, '85) by the in vitro incubation method. Another method of labeling AII amacrine cells in rabbit retina has recently been reported using in vitro incubation in Ames medium after prior intraocular injection with Nuclear Yellow (Gynther et al., '89).

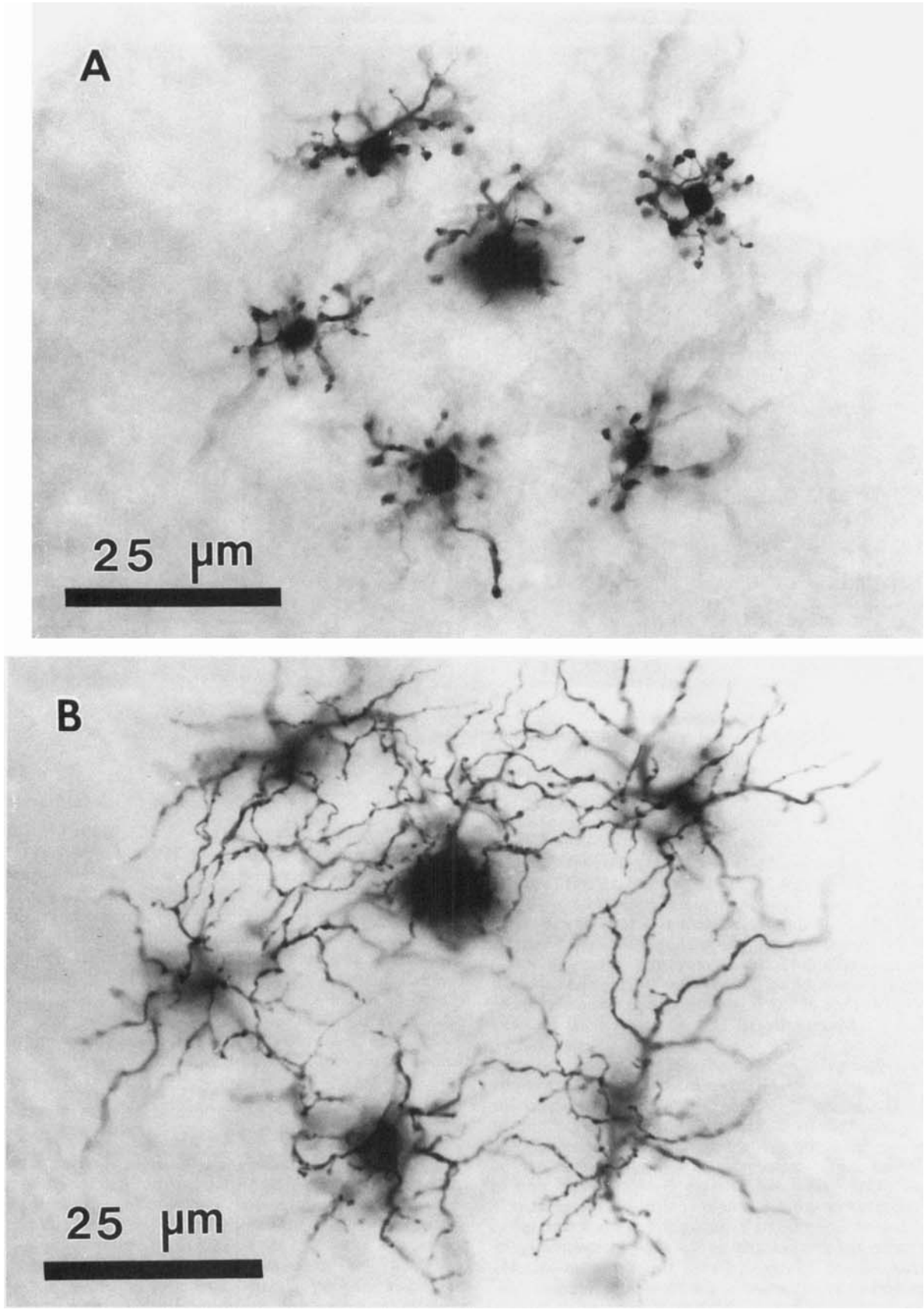

Fig. 4. **(a)** Intracellular injection of Lucifer Yellow into 6 AII amacrine cells reveals the characteristic lobules in sublamina *a*. **(b)** Focusing on sublamina *b* shows the fine processes of the same six AII amacrine cells as in (a).

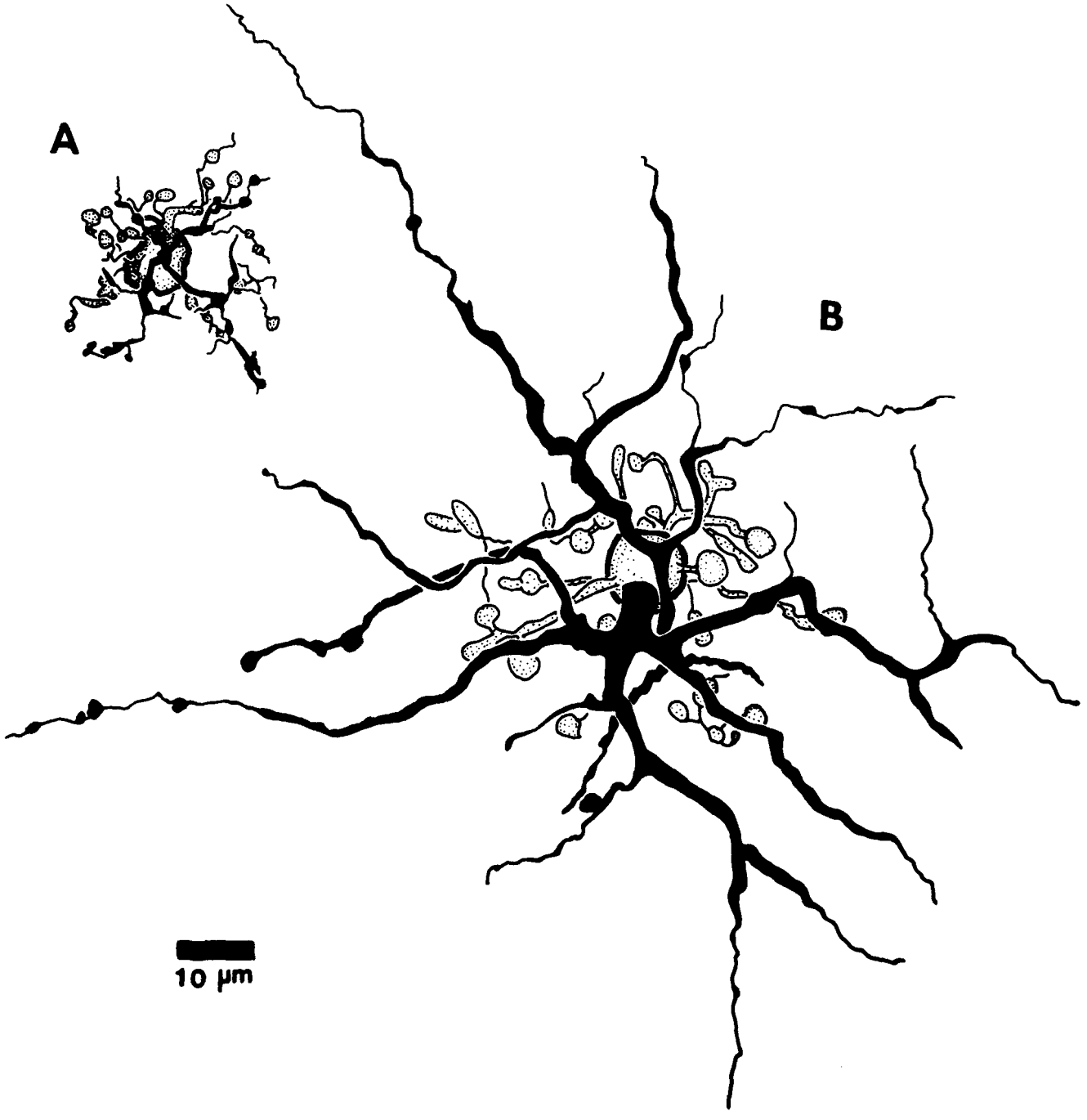

Fig. 5. A comparison of size and morphology of two AII amacrine cells, one from within 2 mm of the visual streak (small cell, left) and the other 10 mm from the central area in the superior retina. The gross difference in size is obvious, but the ratio of the fine dendritic field to the lobular field is much larger in the peripheral cell.

With any labeling procedure, one may reasonably question the extent to which the procedure labels all members of a particular class of cell and to what extent the fluorescent label is taken up by other classes of cell. In vitro incubation of rabbit retina with DAPI leads to a distinct population of AII cells that are easily discriminable by their greater brightness from the background of other cells and by their level of focus. This can be demonstrated by impaling the brightest cells. The lack of false positives, i.e., non-AII amacrine cells, demonstrates that the visible mosaic of bright somas is exclusively one of AII amacrine cells.

The problem of misses, that is, AII amacrine cells not distinct from the background, is more difficult. It is theoretically possible that some AII amacrine cells are dimmer than others and therefore not counted. It is improbable, however, that such cells would take up no dye when their

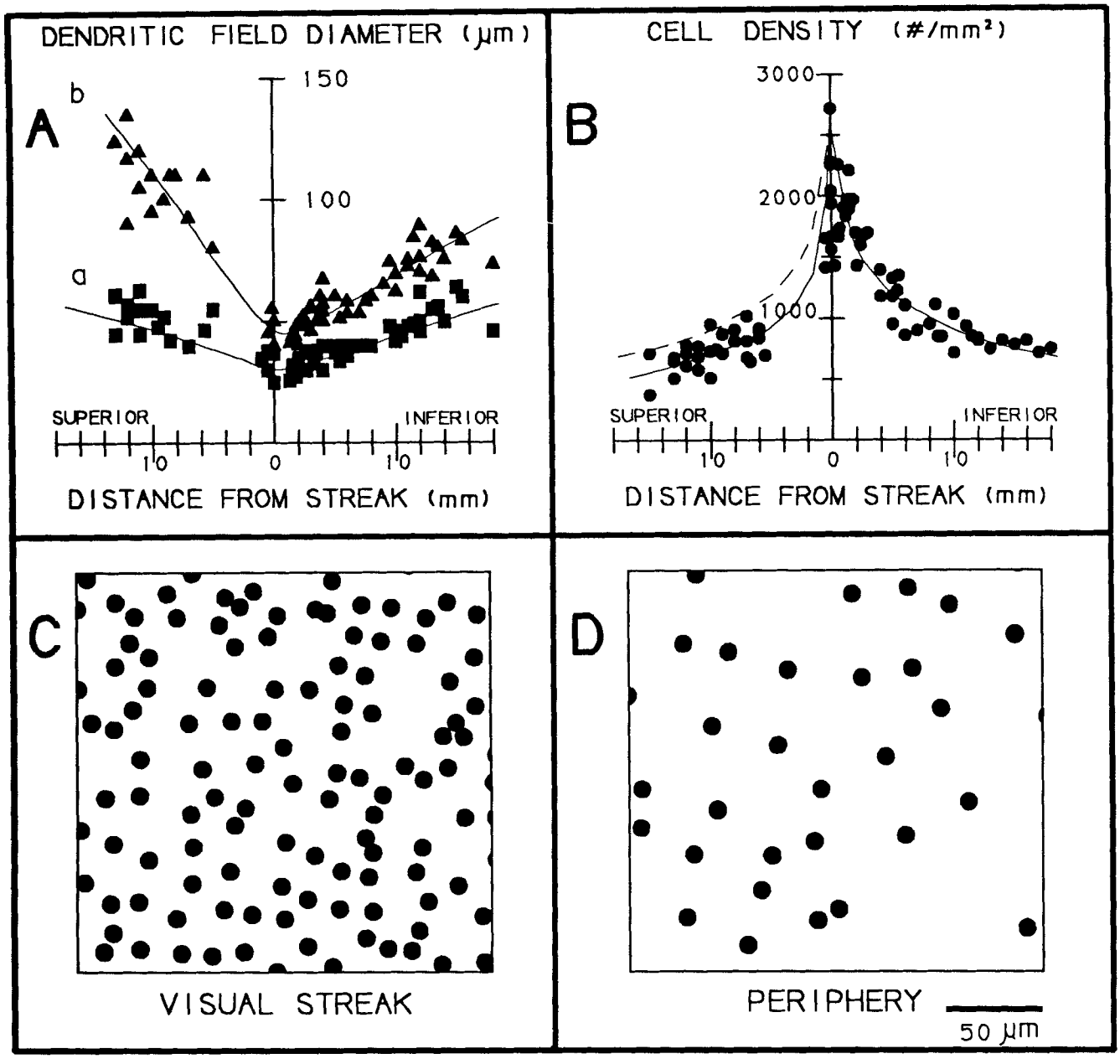

Fig. 6. The size and distribution of AII amacrine cells. **A.** The dendritic field diameter of the lobular appendages in sublamina *a* (a) and the fine processes in sublamina *b* (b) as a function of retinal eccentricity. **B.** Cell density as a function of retinal eccentricity. The dashed line is a reflection about 0° eccentricity of the solid line fitting the data from the inferior retina and shows the more rapid decline in this direction. (**C,D**) Representative samples of AII amacrine cell distribution near the visual streak (C) and 10 mm in the superior periphery (D).

counterparts are so bright. One can assess the extent of this potential problem by impaling and filling cells that are not judged to be AII amacrine cells by their DAPI fluorescence characteristics, but are still visible. The rarity with which these cells prove to be AII amacrine cells is a reassurance of the completeness of labeling.

The extent to which a group of cells can be called a regular mosaic also lends credence to the idea that labeling has been complete and selective. The superposition of a second population of cells would degrade the regular spacing of a single mosaic and would be reflected in low numbers when nearest-neighbor analysis is performed. The relatively high numbers obtained with AII amacrine cells compared to other rabbit amacrine cell populations suggests that labeling is in fact preferential.

DAPI uptake

The mechanism by which DAPI preferentially labels amacrine cells is unknown. DAPI is known to bind to the minor groove of DNA after entry into the cell (Manzini et al., '83). Why DAPI preferentially labels AII amacrine cells in one case and starburst amacrine cells in another is unclear. Possible variables in which cells might differ

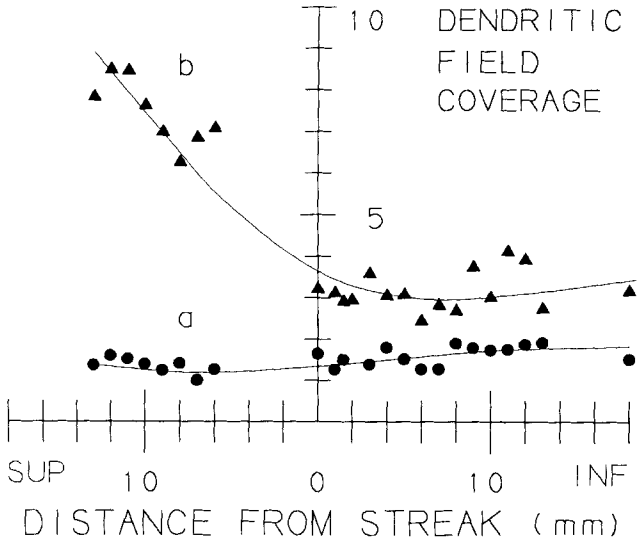

Fig. 7. Dendritic field coverage for AII amacrine cells as a function of retinal eccentricity for the lobular appendages (**a**, filled circles) and the fine processes (**b**, filled triangles).

include rate of diffusion into the cell and affinity for the dye once it has entered the nucleus. It may be that AII amacrine cells are the first to incorporate DAPI, presumably through more rapid initial diffusion into the cell. Starburst amacrine cells, preferentially labeled 2 days after intravitreal injection of low doses of DAPI, may retain DAPI more efficiently. AII amacrine cells, if labeled, are difficult to identify in the INL of retinas injected intraocularly 2 days prior to enucleation. Their lower degree of fluorescence makes them difficult to detect as a regular matrix against the overall background produced by DAPI fluorescence in other amacrine cell types. Nevertheless, it does not seem likely that AII cells merely become undetectable as the background fluorescence rises. Instead, it seems that AII amacrine cells lose their fluorescence over a longer time period. The possibility that they never take up DAPI after intraocular injection can be dismissed by sampling retinas 1–4 hours later. AII amacrine cells are easily found in such preparations, although both the specificity of AII labeling and the variability of labeling across the retina suffer in comparison with the incubation method.

Coverage factors

Coverage factors, calculated by multiplying the density of a cell type by the area of its dendritic field, are taken as a measure of spatial integration. In the cat, the AII amacrine cell shows a decline in cell density with eccentricity, but a corresponding increase in dendritic area per cell (Vaney, '85). The resulting coverage function is very nearly constant for processes in sublamina *a*, with only a minor increase in the periphery in sublamina *b*. In the rabbit, coverage by sublamina *a* processes are again relatively constant at 1.5, but coverage factors calculated for the fine processes in sublamina *b* show a large increase from about 3–4 in the central area and inferior periphery to above 8 in the superior periphery.

The argument has been advanced that spatial integration of widefield cells, such as the starburst and indoleamine-accumulating amacrine cells, may be misrepresented by large coverage factors calculated using cell densities and dendritic areas (Masland '88; Wässle '89). Local dendrites may be the functional units rather than the whole cell. For example, in the central retina, where acuity and ganglion cell density peaks, starburst amacrine cell coverage is at a minimum. If dendritic length/mm^2 is instead plotted, the peak is in the central area, as would be expected. To determine if the high coverage factors found in AII amacrine cells of superior rabbit retina would disappear if dendritic length rather than field area were used as a measure, calculations using dendritic length were made.

Measurement of dendritic length and area in our samples demonstrated that the large coverage factor of the fine processes in the superior retina would indeed be similar to that of the central retina if dendritic length were used instead of dendritic area, with both measuring about 0.6 m/mm^2. The coverage of the inferior retina, however, would fall to about 0.4 m/mm^2. Additionally, the apparent constancy of coverage of the lobular appendages would be lost, changing from 0.16 m/mm^2 in the superior periphery to about 0.30 m/mm^2 in the central and inferior retina.

It appears, then, that whatever constancy is gained in the superior retina by using dendritic length as a measure of coverage is lost in other portions of the retina. It is not surprising that the dendritic length parameter should be less meaningful for AII than for starburst amacrine cells. The dendritic length hypothesis was advanced for application to cells with wide fields and large coverage factors, where the cell may not be the functional unit. The AII amacrine cell, in contrast, has a much smaller field with relatively stout processes and may function largely as a single unit in the traditional sense. The density of cells per unit area is probably an appropriate parameter for measuring coverage.

Distribution and convergence

A comparison of rod pathways in cat and rabbit retinae is now possible. In the cat retina, AII amacrine cells have a peak density of 5,000–6,000 per mm^2 falling to 500 per mm^2 in the periphery (Vaney, 1985). Clearly the AII density is less in the rabbit retina, declining from a maximum near 3,000 per mm^2 in the visual streak to about 500 per mm^2 in the far periphery. In general, rabbit AII amacrine cells have larger dendritic fields, especially in the central retina. Here, in the cat retina, the dendritic field diameter for the lobular appendages is 16 μm and 18 μm for the fine processes in sublamina *b* (Vaney, 1985). The corresponding numbers for the rabbit retina are 25 μm and 40 μm. However, the density and dendritic area combine to give similar coverage factors in both species, around 1 for sublamina *a* and from 3–4 for the fine processes in sublamina *b*. The superior retina of the rabbit is exceptional because the fine processes in sublamina *b* have large dendritic fields with coverage factors around 8.

According to Hughes ('71), photoreceptors in the rabbit retina, mostly rods, reach a peak density of 180,000 per mm^2 in the visual streak. This produces a ratio of 60 rods:2 rod bipolar cells:1 AII amacrine cell at the visual streak. In the cat retina, the corresponding ratios are 110:7:1 for the area centralis (Sterling et al., '88). Thus the cat retina has a greater convergence than the rabbit retina, as well as more cells in the rod pathway. This is consistent with the actual convergence, measured from synaptic contacts, of 20 rod bipolar cells to 1 AII amacrine cell in the cat (Sterling et al. '88), compared to 9 rod bipolar cells to 1 AII amacrine cell in

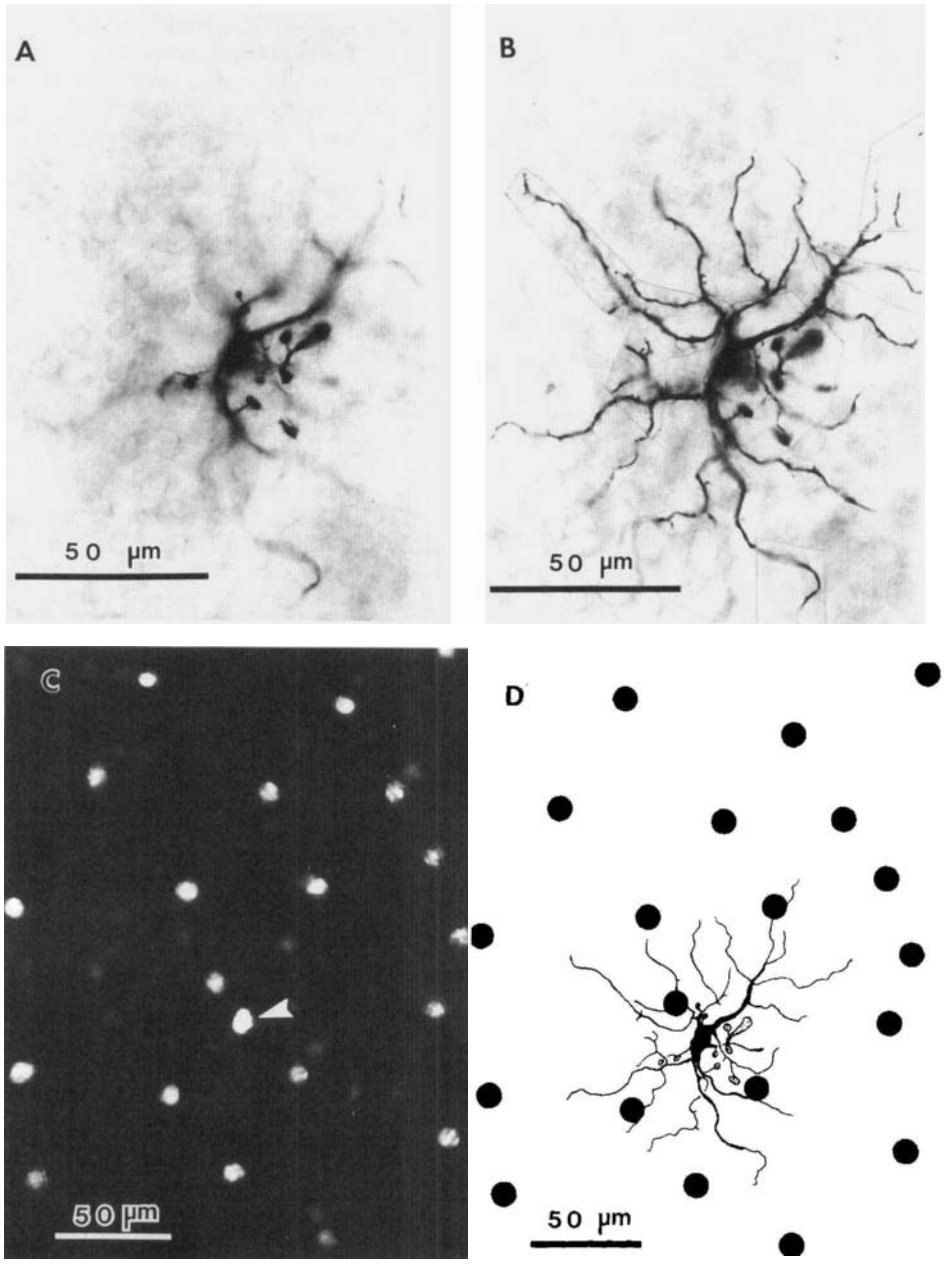

Fig. 8. Dendritic field coverage for a single AII amacrine cell in the superior periphery. **A.** The lobular appendages in sublamina *a*. **B.** The fine processes in sublamina *b*. **C.** The matrix of DAPI cells over the same area. The number of cells within the field of the fine appendages is 6–7; no AII somas overlap the offset field of the lobular appendages. **D.** A simplified line drawing comparing the dendritic spread of the cell with the placement of adjacent AII amacrine cell somas.

the rabbit (Strettoi et al., '89). Convergence is steep in both the cat and rabbit retina; this may be a characteristic of rod systems designed to increase sensitivity.

Comparisons with other species

Bistratified amacrine cells were originally described by Cajal (1892) in nonmammalian retinas. Since then, narrow-field bistratified amacrine cells have been found in the primate (Polyak, '41; Boycott and Dowling, '69), as well as the cat (Vaney, '85), rat, and rabbit retinae (Perry and Walker, '80; Voigt and Wässle, '87). The retina of the marsupial wallaby also contains the AII amacrine cell type (Wong et al., '86). The close similarity of the bistratified amacrine cells in these species suggests that this cell type is well conserved across species, presumably due to its critical role in the rod pathway.

ACKNOWLEDGMENTS

The authors thank Kevin Blankenship for excellent technical work on this project and Robert E. Marc for invaluable advice and assistance. This project was supported by NEI grant EY-06515 and Texas Higher Education Coordinating Board Grant 1953 to S.C.M. and NEI training grant EY-07024 to S.L.M.

LITERATURE CITED

Ames, A. III and F.B. Nesbett (1981) *In vitro* retina as an experimental model of the central nervous system. J. Neurochem. *37:*867–877.

Boycott, B.B., and J.E. Dowling (1969) Organization of the primate retina: Light microscopy. Phil. Trans. R. Soc. Lond. B *255:*109–184.

Cajal, S. Ramón y (1892) Le rétine des vertébrés. La Cellule.

Dacheux, R.F., and E. Raviola (1986) The rod pathway in the rabbit retina: Depolarizing bipolar and amacrine cell. J. Neurosci. *6:*331–345.

Famiglietti, E.V. Jr., and H. Kolb (1975) A bistratified amacrine cell and synaptic circuitry in the inner plexiform layer of the retina. Brain Res. *84:*293–300.

Gynther, I.C., H.M. Young, and D.I. Vaney (1989) Topographic relationships between rod-signal interneurons in rabbit retina. Abstract, Society for Neuroscience, 19th meeting, Phoenix, AZ.

Hughes, A. (1971) Topographical relationships between the anatomy and physiology of the rabbit visual system. Doc. Ophthalmol. *30:*33–159.

Karnovsky, M.J. (1971) Use of ferrocyanide-reduced osmium tetroxide in electron microscopy. In: Proceedings of the 11th Annual Meeting, American Society for Cell Biology, New Orleans, p. 146a.

Kolb, H., and E.V. Famiglietti Jr. (1974) Rod and cone pathways in the inner-plexiform layer of cat retina. Science *186:*47–79.

McGuire, B.A., J.K. Stevens, and P. Sterling (1984) Microcircuitry of bipolar cells in cat retina. J. Neurosci. *4:*2920–2938.

McGuire, B.A., J.K. Stevens, and P. Sterling (1986) Microcircuitry of beta ganglion cells in cat retina. J. Neurosci. *6:*907–918.

Manzini, G., M.L. Barcellona, M. Avitabile, and F. Quadrifoglio (1983) Interaction of diamidino-2-phenylindole (DAPI) with natural and synthetic nucleic acids. Nucleic Acids Res. *11:*8861–8876.

Maranto, A. (1982) Neuronal mapping: a photooxidation reaction makes Lucifer Yellow useful for electron microscopy. Science *217:*953.

Masland, R.H. (1988) Amacrine cells. TINS *11:*405–410.

Masland, R.H., J.W. Mills, and S.A. Hayden (1984) Acetylcholine-synthesizing amacrine cells: identification and selective staining by using radioautography and fluorescent markers. Proc. R. Soc. Lond. B *223:*79–100.

Nelson, R. (1982) AII amacrine cells quicken time course of rod signals in the cat retina. J. Neurophysiol. *47:*928–947.

Perry, V.H., and M. Walker (1980) Amacrine cells, displaced amacrine cells and interplexiform cells in the retina of the rat. Proc. R. Soc. Lond. B *208:*415–431.

Polyak, S.L. (1941) The retina. Chicago: University of Chicago Press.

Pourcho, R.G., and D.J. Goebel (1985) A combined Golgi and autoradiographic study of [^{3}H]glycine-accumulating amacrine cells in the cat retina. J. Comp. Neurol. *233:*473–480.

Pourcho, R.G., and D.J. Goebel (1987) Visualization of endogenous glycine in cat retina: an immunocytochemical study with FAB fragments. J. Neurosci. *7:*1189–1197.

Raviola, E., and R.F. Dacheux (1987) Excitatory dyad synapse in rabbit retina. Proc. Natl. Acad. Sci. USA *84:*7324–7328.

Sandell, J.H., and R.H. Masland (1986) A system of indoleamine-accumulating neurons in the rabbit retina. J. Neurosci. *6:*3331–3347.

Sandell, J.H., and R.H. Masland (1988) Photoconversion of some fluorescent markers to a diaminobenzidine product. J. Histochem. Cytochem. *36:*555–559.

Sterling, P. (1983) Microcircuitry of the cat retina. Ann. Rev. Neurosci. *6:*149–185.

Sterling, P., M.A. Freed, and R.G. Smith (1988) Architecture of rod and cone circuits to the on-beta ganglion cell. J. Neurosci. *8:*623–642.

Stewart, W.W. (1981) Lucifer dyes—highly fluorescent dyes for biological tracing. Nature *292:*17–21.

Strettoi, E., R.F. Dacheux, and E. Raviola (1990) Synaptic connections of rod bipolar cells in the inner plexiform layer of the rabbit retina. J. Comp. Neurol. *295:*449–466.

Strettoi, E., E. Raviola, and R.F. Dacheux (1989) Synaptic connections of AII amacrine cells in the rabbit retina. Abstract, Society for Neuroscience, 19th meeting, Phoenix, AZ.

Tauchi, M., and R.H. Masland (1984) The shape and arrangement of the cholinergic neurons in the rabbit retina. Proc. R. Soc. Lond. B *223:*101–119.

Vaney, D.I. (1984) "Coronate" amacrine cells in the rabbit retina have the 'starburst' dendritic morphology. Proc. R. Soc. Lond. B *220:*501–508.

Vaney, D.I. (1985) The morphology and topographic distribution of AII amacrine cells in the cat retina. Proc. R. Soc. Lond. B *224:*475–488.

Voigt, T., and H. Wässle (1987) Dopaminergic innervation of AII amacrine cells in mammalian retina. J. Neurosci. *7:*4115–4128.

Wässle, H. (1989) Horizontal cells in the monkey retina: Cone connections and dendritic network. Eur. J. Neurosci. *1:*421–435.

Wässle, H., and H.J. Riemann (1978) The mosaic of nerve cells in the mammalian retina. Proc. R. Soc. Lond. B *200:*441–461.

Wässle, H., I. Schäfer-Trenkler, and T. Voigt (1986) Analysis of a glycinergic inhibitory pathway in the cat retina. J. Neurosci. *6:*594–604.

Wong, R.O.L., G.H. Henry, and C.J. Medveczky (1986) Bistratified amacrine cells in the retina of the tammar wallaby—*Macropus eugenii*. Exp. Brain Res. *63:*102–105.